A Numerical Study on the Effects of Environmental Flow on Tropical Storm Genesis

ROBERT E. TULEYA AND YOSHIO KURIHARA

Geophysical Fluid Dynamics Laboratory/NOAA, Princeton University, Princeton, NJ 08540

(Manuscript received 3 August 1981, in final form 19 October 1981)

ABSTRACT

The role of the environmental wind in tropical storm genesis is studied using a numerical simulation model. The model used is an 11-level, primitive equation model covering a channel domain of 25° span with open lateral boundaries at 5.5 and 30.5°N. A number of experiments were integrated for 96 h in which the initial zonal mean flow was specified differently. The superposed initial wave disturbances were identical in all experiments.

The dynamic coupling between the upper-level winds and the low-level movement of the disturbance was found to be an important factor in explaining the role of the environmental wind in storm genesis. Another important factor is the impact of the low-level winds on the latent energy supply. This supply is affected by the relative inflow into a disturbance and by the transfer of momentum from aloft into the boundary layer in a large area surrounding the disturbance.

According to the model results, the storm genesis potential is definitely biased toward easterly vertical shear (easterlies increasing with height) of the environmental flow rather than westerly shear when the mean surface flow is easterly, i.e., -5 m s^{-1}. The initial perturbation developed into a vigorous tropical storm when an easterly vertical shear of 15 m s^{-1} was specified between 150 and 850 mb. In an experiment with a specified westerly vertical wind shear of 15 m s^{-1}, the perturbation failed to develop beyond a weak tropical depression. In a third experiment with no vertical wind shear but with anticyclonic shear aloft, a tropical storm also developed. In analyzing the structure of the disturbances at the early wave stage it was found that the vertical shear modulated the vertical velocity and rainfall patterns relative to the trough axis.

In studies involving the horizontal wind shear of the basic flow, it was found that cyclonic shear at low levels and, to a lesser extent, anticyclonic shear at upper levels are conducive for storm genesis. The experimental results also indicate a significant change of structure of the disturbance between uniform westerly and easterly flows. Under uniform westerly environmental flow, the initial perturbation developed more and its low-level structure became more characteristic of mid-latitude cyclones.

1. Introduction

The development of a weak atmospheric tropical disturbance into a tropical depression, then to a tropical storm, and perhaps into a typhoon or hurricane, is termed storm genesis. Genesis is characterized by the weak disturbance, such as an easterly wave or cloud cluster, attaining an upper-level warm core and increasing its low-level vorticity by an order of magnitude. The fact that very few of these weak disturbances develop into tropical storms has been of great interest in both operational and research fields. Undoubtedly, the degree of development of a disturbance is influenced by many factors. The internal dynamics and thermodynamics of the disturbance itself are important to its future existence. These thermodynamic mechanisms involve cloud-scale processes such as interaction among clouds, and the ensemble effect of clouds on the disturbance-scale circulation. Research has begun on this intriguing subject (e.g., Yamasaki, 1977).

On the other hand, the external influence of the environmental flow on the behavior of a weak disturbance is another fascinating problem. One obvious impact of the surrounding environmental flow is its steering influence on the track of the disturbance. Another more subtle, less understood effect of the environmental flow is its impact on the possible intensification of a disturbance into a tropical storm. Much research has been performed to investigate the necessary environmental flow conditions for storm development (see Kurihara and Tuleya, 1981, Section 1). One common problem involved in such studies is the inability to define the disturbance with absolute accuracy. In reality, the disturbance and its environmental flow intermingle. Because of this natural ambiguity, the environmental flow has different connotations. Often environmental flow is defined as some zonal mean state over a specified longitudinal extent at a specified latitude, or alternatively, a time mean over a specified region. A definition often used in case studies or composite analyses is the immediate flow which surrounds the incipient storm itself.

The present study's numerical approach is an extension of the work by Kurihara and Tuleya (1981, hereafter referred to as KT) in which simple envi-

ronmental flows are superposed on a shallow perturbation resembling an easterly wave. One obvious advantage of this approach is the ability to change one environmental flow parameter at a time while the basic thermal, moisture and perturbation fields are fixed. In this numerical study, the same perturbation flow field is used in the initialization of each experiment. At least initially, there is no ambiguity about the mathematical distinction between disturbance and environment. The various environmental flows defined in the series of experiments in this study are rather simple with the hope that storm-environment interactions may be more easily understood.

In the present paper, the numerical model used is described briefly in Section 2. In Section 3, the experimental design is explained. Four different series of experiments are performed. Detailed investigations of the evolution history and the budgets of vorticity, heat and energy are made for four selected cases having different environmental flow conditions. These analysis results are presented and compared with each other in Sections 4 and 5. Discussions are focused on the effect of vertical wind shear on tropical storm genesis in Section 6, and on the effects of horizontal wind shear and uniform mean flow in Section 7. Finally, a summary and remarks are presented in Section 8.

2. Description of the model and review of the control experiments

a. Model description

The 11-level, primitive equation model used in the present study is identical to that described by KT. The model is a channel-type with a 25° × 25° domain centered at 18°N. Parameterization of subgrid-scale processes include the convective scheme by Kurihara (1973) and a vertical mixing scheme described by Mellor and Yamada (1974). The model is a uniform grid version of that described by Kurihara and Bender (1980) with the inclusion of a simple radiative scheme. The resolution of the model is ⅝° latitude and longitude with cyclic boundary conditions at the east–west boundaries and open boundaries at the north and south extremities of the domain. Only the initial conditions involving the basic flow were changed from one experiment to another. Each experiment was integrated 96 h from the specified initial conditions.

b. Review of previous results

In a recent study with the abovementioned model, a simulation of the genesis of a tropical storm from an easterly wave was performed by KT. The primary experiment (Exp. 1) gave a rather realistic simulation involving an increase of maximum surface winds from <8 m s^{-1} to a maximum of ~ 18 m s^{-1}. A corresponding increase of vorticity occurred with values increasing from 4.3×10^{-5} to 23.7×10^{-5} s^{-1} at model level 9($\sim$950 mb) as the disturbance decreased in size. The development of a warm core at $\sim$330 mb and an associated upper-level anticyclone highlighted this experiment. The initial conditions of the basic flow were an idealized version of the GATE III period flow field at 80°W characterized by small vertical wind shear and low-level cyclonic horizontal shear and assumed constant in the longitudinal direction. The basic-state temperature and moisture were based on a six-station average along 80°W for this period. The sea surface temperature was fixed at 302 K (28.8°C). A basic state similar to GATE III was selected as the initial conditions for Exp. 1 because this period was an active one for storm activity. However, the spacial and temporal variations of the basic state as well as differences in the incipient disturbances themselves undoubtedly contributed to the selection process by which some waves developed while some did not.

Besides Exp. 1, two other experiments were described in KT. Exp. 2 indicates the twofold role of radiation in genesis. Differential heating rates between the cloud and cloud-free areas produce a net relative heating in the cloud region and enhance the warm core formation and the associated solenoidal field. Another destabilization effect of radiation is caused by net atmospheric cooling relative to a fixed sea surface temperature. Exclusion of these radiational effects caused the disturbance in Exp. 2 to develop at a slower rate and to a lesser degree than in Exp. 1. This result is in agreement with that of Sundqvist (1970). Exp. 3 was a dry version of Exp. 1 and illustrates the dramatic and crucial role moisture and moisture supply from the ocean play in storm genesis. The time history of the three experiments' maximum surface wind are presented in Fig. 1.

3. Experimental design

In order to investigate the role of different environmental winds on the genesis of a tropical storm, a number of experiments were performed with different initial basic flows. In each of these experiments the initial basic reference temperature and mass, i.e., those at the center latitude, and the relative humidity field were identical to the control experiment (Exp. 1) described in KT. In addition, the initial disturbance was the same for all experiments, i.e., a shallow sinusoidal wave of 25° wavelength, with no vertical or horizontal tilt of axis. The vertical and meridional profiles of the wave amplitude are illustrated in Fig. 2. [For further detail, see Eqs. (3.2), (3.3) and (3.4) in KT.] Notice that the perturbation is initially confined below $\sigma = 0.365$ (σ is the pressure normalized by the surface value) and to within 8.5° latitude of

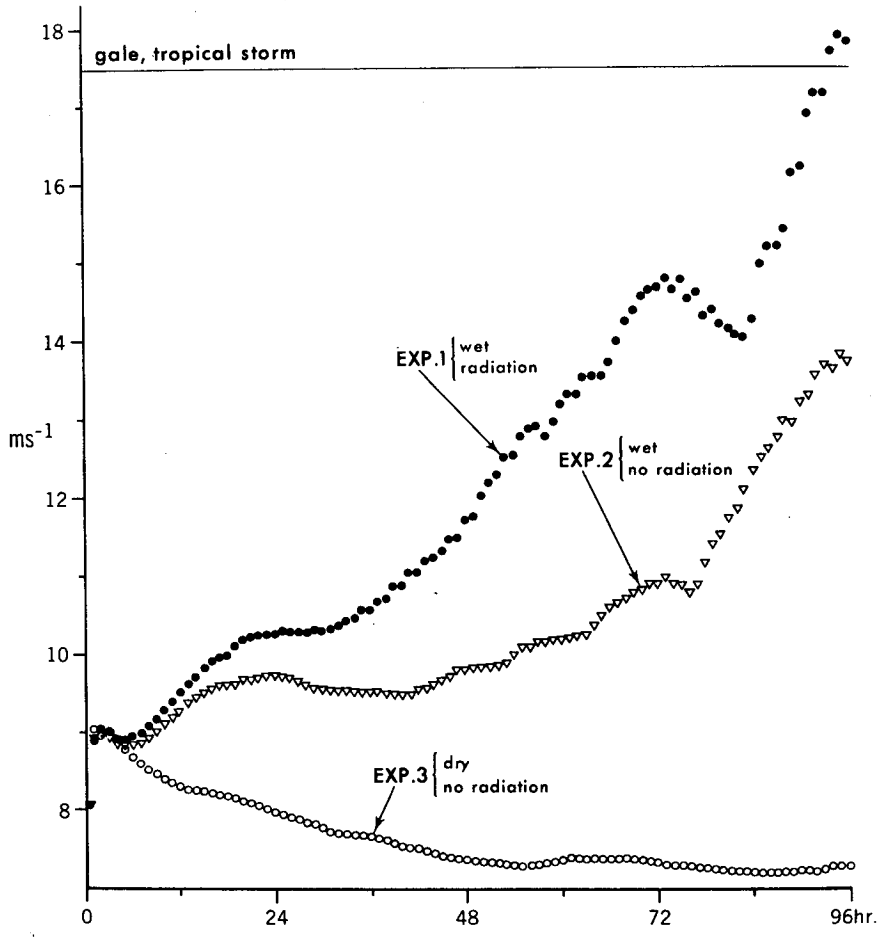

FIG. 1. Time variation of maximum surface wind of the primary disturbance in Exps. 1, 2 and 3.

the domain center. The maximum perturbation magnitude is 5 m s^{-1}.

The initial basic environmental flow is defined as

$$\bar{u}(\sigma, \phi) = u_0(\sigma)\frac{\cos\phi}{\cos\phi_0} - u_1(\sigma)\tanh\left(\frac{\phi - \phi_0}{D}\right), \quad (3.1)$$

where ϕ is the latitude, ϕ_0 the center latitude (18°N) of the channel and D is specified as 2.5° latitude. The first term on the right in (3.1) describes the component of the basic flow with constant angular velocity and the second term describes the variation on the basic flow with latitude. Positive and negative values of u_1 yield, respectively, cyclonic and anticyclonic horizontal shear. The basic flow at the center latitude is equal to $u_0(\sigma)$.

The experiments were performed with various combinations of u_0 and u_1 profiles. Generally, the selection rationale of the experiments performed are such that they are similar to Exp. 1 and still relatively realistic. Except for a few experiments, all exhibit similarities to Exp. 1 in that low-level cyclonic shear and/or an easterly surface flow are specified. They are grouped into four series as shown schematically in Fig. 3. In experimental series A, u_1 is fixed to a positive constant and the profile of u_0 is changed. At low levels the flow field is identical to Exp. 1. The vertical shear is uniform with respect to latitude. Series A is designed to study the role of the vertical shear of the basic environmental flow. In series B experiments, either or both of the low-level cyclonic shear and upper-level anticyclonic shear which were present in Exp. 1 are removed so that the influence of horizontal shear can be examined. This is achieved by changing the profile of u_1 while u_0 is fixed at the same constant as the one used in Exp. 1. The role of horizontal shear also is investigated in series C, which consists of the experiments with u_0 and u_1 both fixed with height. In this series, horizontal shears do not change with height and vertical shears do not exist anywhere. Through experimental series D, the effect of a uniform basic flow on the evolution of a

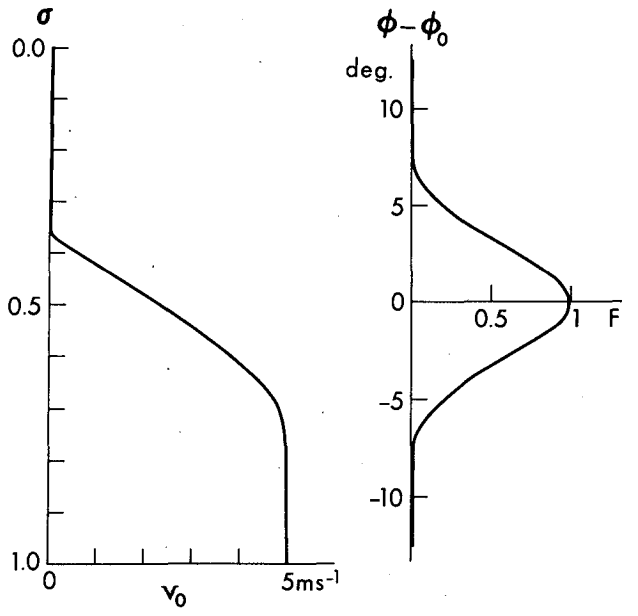

FIG. 2. Vertical variation of perturbation amplitude at the center latitude ϕ_0, 18°N (left) and meridional profile of the ratio of perturbation amplitude to maximum amplitude (right). These parameters determine the amplitude of the initial wave disturbance.

disturbance is discussed. In this case, u_1 is set to zero and different constants are assigned to u_0.

In addition to Exp. 1, three experiments, designated as Exps. 4, 5 and 6, respectively, are indicated by marks other than a cross in Fig. 3. In the following two sections, detailed analyses and comparison of these four experiments are presented in order to highlight the effects of vertical and horizontal shear of the basic flow on the development of a disturbance. Then, more general discussions on the influence of the environmental flow on storm genesis are made in Sections 6 and 7 based on the results of all experiments in the four series.

4. Evolution of a disturbance under four different environmental conditions

a. Four different basic flows

In this section, differences among some synoptic features of Exps. 1, 4, 5 and 6 are studied. The initial mean zonal winds, i.e., the basic flows, of these experiments are presented in the top half of Fig. 4. Exp. 4 has a uniform easterly flow of ~ -5 m s^{-1} throughout the channel. No shear, horizontal or vertical, exists in this case. In Exp. 5, the low-level basic flow is identical to Exp. 1, but from approximately 850 to 150 mb a westerly shear of 15 m s^{-1} is imposed at all latitudes. The magnitude of this shear is similar to observations during GATE I and II in the Caribbean (Sadler and Oda, 1980). Exp. 6 is identical to Exp. 5 except the imposed shear is opposite in sign, that is, an easterly shear of 15 m s^{-1} is specified. Climatologically, easterly shear exists during the hurricane season in parts of the Gulf of Mexico and the equatorial Atlantic genesis regions. Some regions of the western North Pacific, the South China Sea, and the Indian Ocean and Bay of Bengal also exhibit easterly vertical shears during the tropical cyclone season (Gray, 1968; Keshavamurty *et al.*, 1978).

b. Time history of the four experiments

The disturbance tracks of Exp. 1 together with those of Exps. 4, 5 and 6 are shown in Fig. 5. Along each track, the positions of the disturbance (determined from a surface pressure chart), the minimum surface pressure, and the maximum vorticity at level 9 (~950 mb) are indicated at 24 h intervals. The disturbance in Exp. 1, as discussed in KT, moved toward the west-northwest at 6° longitude day^{-1} and developed into a tropical storm. The disturbance in the uniform flow case (Exp. 4) has a similar track to Exp. 1 with slightly slower movement, but did not develop beyond a tropical depression. The disturbance superposed upon the basic flow with westerly vertical shear (Exp. 5) exhibited little intensity change. After 96 h, a weak tropical depression existed with a central surface pressure approximately only 1.5 mb lower than its initial pressure. Notice that its westward movement is ~4° longitude day^{-1}, obviously retarded by the westerlies aloft. In contrast to Exp. 5, the disturbance within the easterly vertical shear in Exp. 6 moved toward the west at 9° longitude day^{-1}. As the disturbance moved rapidly westward, it developed sooner and to a more intense state than Exp. 1. Notice that at 24 h, the central pressures of all four experiments were within 0.5 mb of one another, but the maximum vorticity values ranged from 41 to 56 $\times$ 10^{-6} s^{-1}.

The time history of the maximum surface wind is shown in Fig. 6. Both the disturbances in Exps. 1 and 6 develop into tropical storms with maximum surface winds of ~18 and ~23 m s^{-1}, respectively. The winds in the disturbance in Exp. 5 do not exceed 12 m s^{-1} and decay after 60 h. The maximum winds in the disturbance of Exp. 4 are initially weaker than the other experiments because of the initial lack of horizontal shear. The maximum winds in this case show a slow gradual increase to ~10 m s^{-1} at 96 h. Notice that in the cases with identical low-level initial conditions (Exps. 1, 5 and 6) the maximum surface winds remain practically identical until ~36 h while a similar tendency is noticed in the central surface pressure. Initially, none of the four experiments exhibit any upper-level (~335 mb) warm anomalies. By 48 h, warm anomalies form above the disturbances in Exps. 1 and 6. In the westerly vertical shear case (Exp. 5) no significantly warm areas are directly associated with the main disturbance

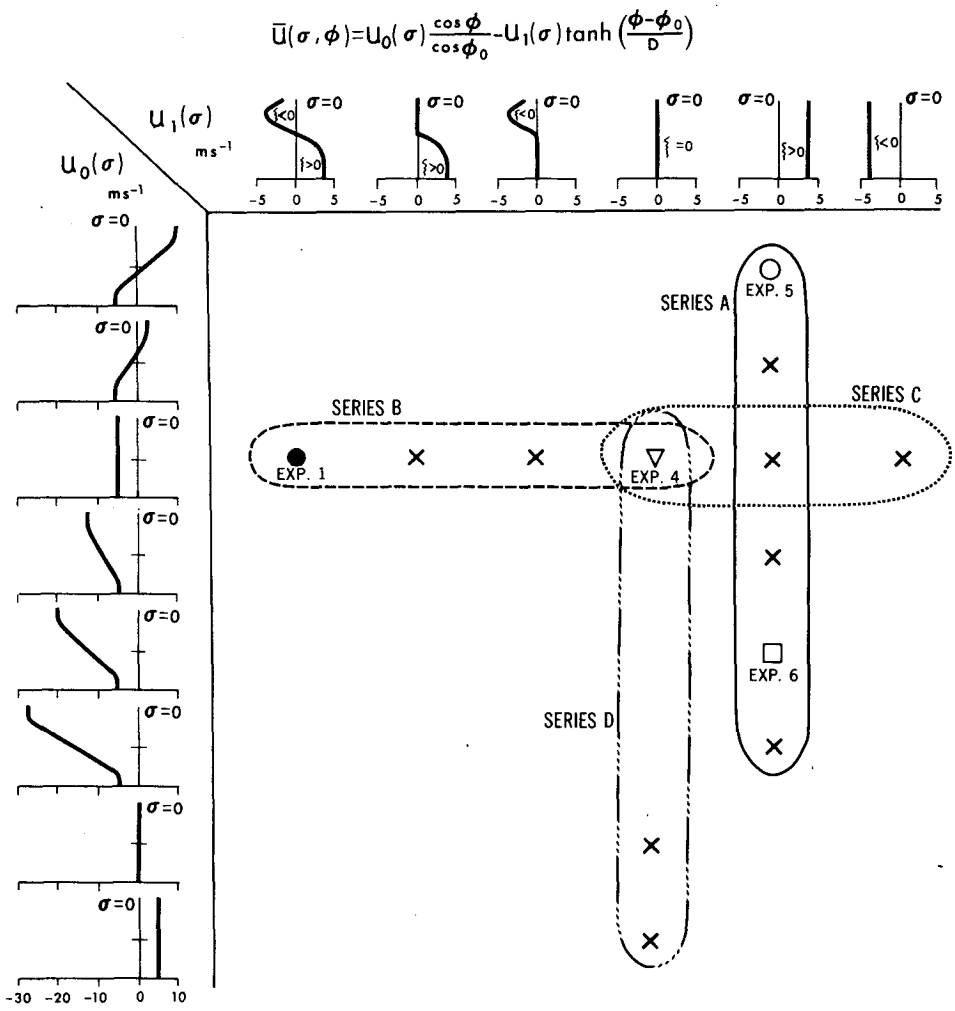

FIG. 3. Diagram showing each experiment and each experimental series in this study as a function of u_0 and u_1. The horizontally uniform part (angular velocity constant) of the environmental flow is defined as u_0. The horizontally nonuniform part of the environmental flow is defined at u_1.

throughout the 96 h period. Table 1 summarizes the results of the experiments at 96 h. There is clearly a directional bias toward easterly shear or no vertical shear in the genesis tendencies in the four experiments. Westerly vertical shear which is exhibited in Exp. 5 obviously retarded the growth of the disturbance. The lack of cyclonic horizontal shear of the environmental flow, described in Exp. 4, also had a detrimental effect on storm genesis.

c. *Comparative analysis of vorticity and rainfall distributions at 24 h*

As previously mentioned, one sees little surface pressure differences among the four experiments before 36 h. The disturbances in Exps. 1, 5 and 6 also indicate little differences in maximum surface winds at 36 h. However, some significant differences among the four experiments can be seen in the low-level vorticity and rainfall distributions as early as 24 h. Distributions of these quantities are shown by broken and solid lines, respectively, in the top half of Fig. 7. The thick solid lines in the figure indicate trough positions. An even more enlightening analysis is the corresponding difference from Exp. 1 shown in the bottom half of Fig. 7. In Exp. 1, the maximum rainfall area is to the north of the surface pressure center, and to the west of the trough axis. The maximum vorticity area is also displaced to the north of the surface pressure minimum by approximately 2° latitude. In the uniform flow case (Exp. 4) the magnitudes of the low-level vorticity and rainfall are reduced. The precipitation pattern is positioned to the east of that of Exp. 1 and centered near the trough axis. Fig. 7 shows that the vorticity patterns of Exps. 5 and 6 are similar to that of Exp. 1 but subtle position changes occur relative to the location of surface pressure minimum. As a result, the developing case

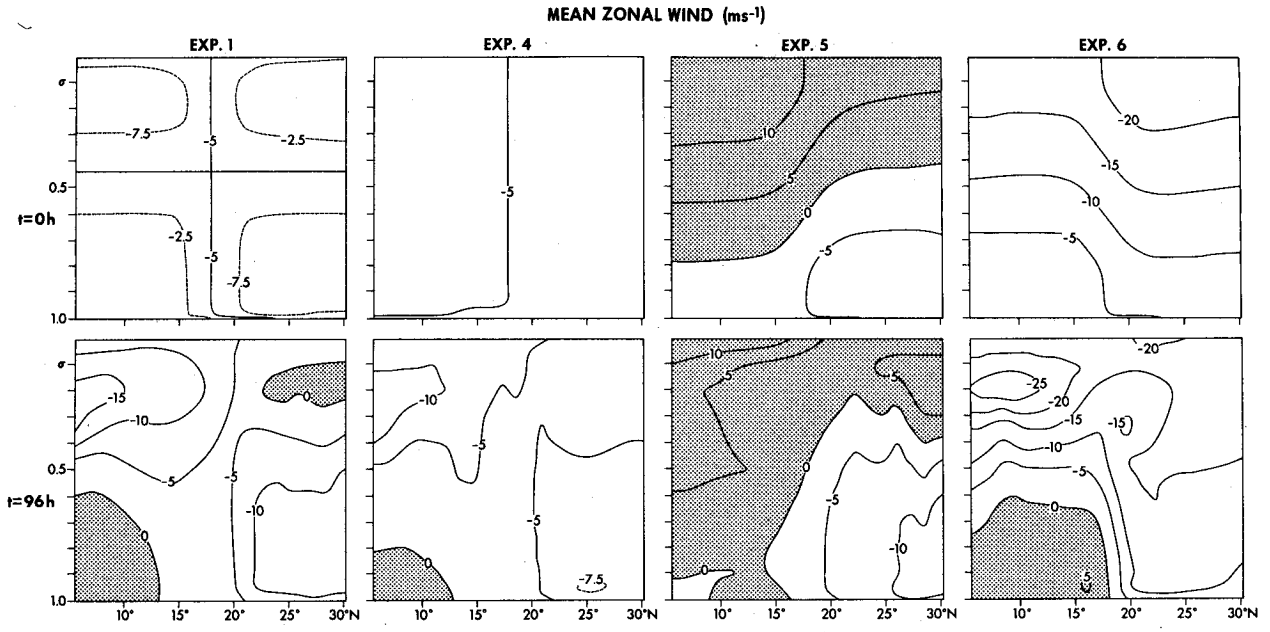

FIG. 4. Latitude-height distributions of the longitudinal mean of the zonal flow at 0 h (top, m s^{-1}) and 96 h (bottom, m s^{-1}) for Exps. 1, 4, 5 and 6. Shading indicates positive, or westerly component of the mean zonal wind.

(Exp. 6) indicates a positive departure of vorticity relative to Exp. 1 at the disturbance center, while that of Exp. 5, the non-developing case, indicates a negative departure. Therefore, despite similar intensities of surface wind and surface pressure with Exp. 1, significant vorticity departures are created near the center. Another structural difference between Exp. 1 and Exps. 5 or 6 is manifested in the rainfall distributions. The shading in Fig. 7 indicates a positive departure of rainfall relative to Exp. 1. The non-developing disturbance in Exp. 5 exhibits a rainfall pattern more like the classical easterly wave model with a rainfall maximum to the east of the trough. In the developing disturbance of Exp. 6, the large rainfall is confined to west of the trough axis. The modulation of rainfall patterns by the vertical wind shear in tropical waves was discussed by Riehl (1954) and implied by the diagnostic study of Holton (1971).

d. Comparative analysis of wind fields

Low-level streamline analyses were performed for the four experiments at 24 h intervals. This is shown in Fig. 8. Initial streamlines in Exps. 1, 5 and 6 are identical, but in Exps. 1 and 6 there occurs a spin-up of the wave into a small intense vortex by 96 h. The disturbance of Exp. 5 in an environmental westerly shear of 15 m s^{-1}, however, exists as a broad, weak tropical depression with little intensity change from 24 to 72 h before weakening. Also interesting is the appearance of a secondary circulation to the southwest of the principal system in Exps. 1 and 4. Fig. 9 shows the streamlines at level 4 (~335 mb) at 24 h intervals for the four different experiments. As explained in KT, the development of an upper-level anticyclonic flow in conjunction with the protrusion of a small cyclonic area near the storm center was observed in Exp. 1. A similar feature appears in Exp. 4, but the wind speed is much less than that of Exp. 1. The development of a cyclonic-anticyclonic flow pair immediately northeast of the surface disturbance highlights the upper level flow in Exp. 5. This flow is consistent with and apparently caused by the downstream propagation of the effect of twisting of the horizontal vorticity associated with the westerly vertical wind shear. The transition line between cyclonic and anticyclonic flow is north of the storm center and more or less coincident with the line of strong upward motion. In the case of the easterly wind shear (Exp. 6) anticyclonic curvature is found to the southwest of the storm center at 48 h. In Exp. 6, a protrusion of the developing low-level vortex appears near the storm center in a similar fashion to Exp. 1.

e. Change of mean zonal wind

As the finite-amplitude disturbance evolves and interacts with the mean zonal winds, the zonal wind obviously changes with time. The mean zonal winds at 96 h for Exps. 1, 4, 5 and 6 are shown in the bottom half of Fig. 4. In the development cases (Exps. 1 and 6) both lower-level cyclonic shear and upper-level anticyclonic shear are increased because of the genesis of a strong vortex. Exp. 4 had an initial

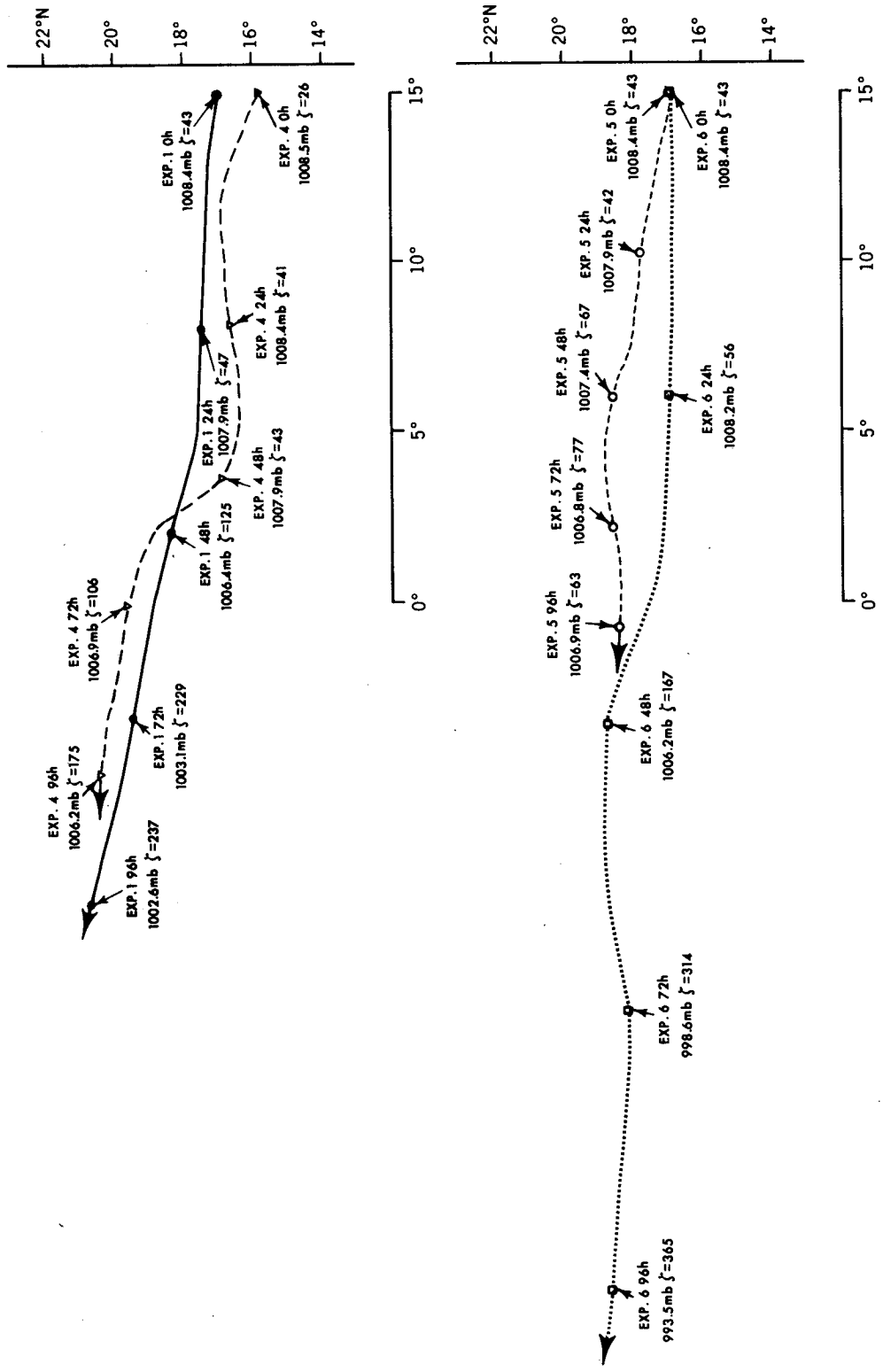

FIG. 5. Storm track of major disturbances in Exps. 1 and 4 (top) and Exps. 5 and 6 (bottom). Positions are plotted every 24 h with central pressure and level 9 ($\sigma = 0.95$) vorticity (10^{-6} s^{-1}) at disturbance center indicated.

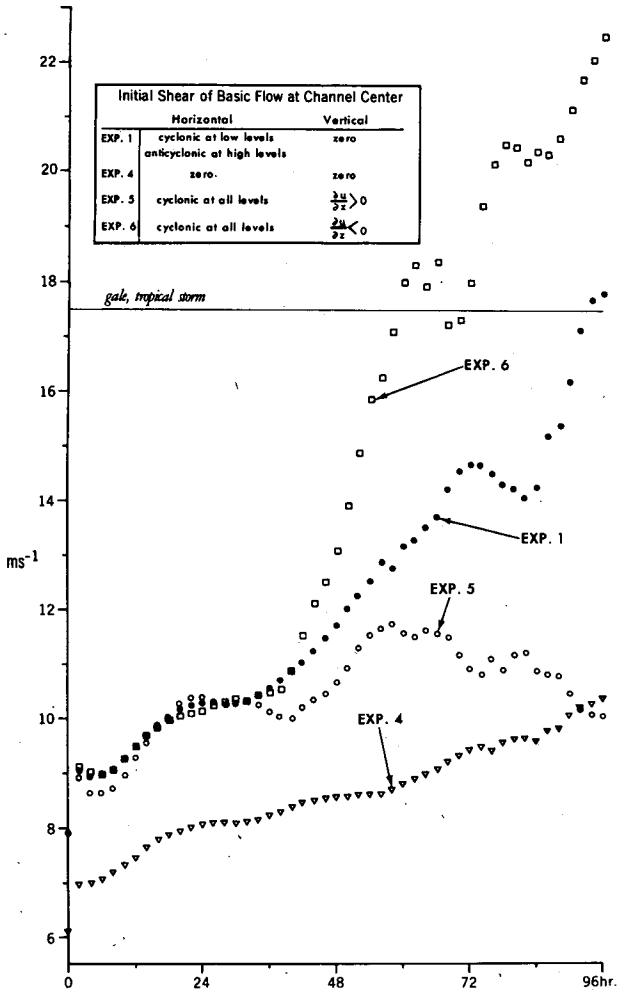

FIG. 6. Time variation of maximum surface wind of the primary disturbances in Exps. 1, 4, 5 and 6.

basic flow with a uniform angular rotation rate. In this case as well, there is a tendency for more cyclonic shear in the lower troposphere and more anticyclonic shear aloft. In Exp. 5, the deviation of mean zonal wind at 96 h from the initial condition reflects development of the flow patterns as shown in Figs. 8 and 9.

It should be noted here that, in the present model, the zonal mean temperature field was forced weakly toward the initial state in the same manner as the one used in KT. Such a condition should affect the evolution of the mean zonal wind to a certain degree.

5. The vorticity, heat and energy tendencies under four different environmental conditions

a. Vorticity tendency

The vorticity budgets were analyzed for Exps. 4, 5 and 6 in an identical manner to those for Exp. 1 as reported by KT. The longitude-height distributions of the net vorticity tendencies at 24 and 48 h for all four experiments are shown in Fig. 10. These cross sections are taken through the position of surface pressure minimum. The computed net tendencies represent quasi-Lagrangian tendencies, i.e., the time change viewed from the reference frame which is fixed to the moving disturbance.

At 24 h, the net positive tendency regions for the developing cases (Exps. 1 and 6) are closer to the center than for the non-developing case (Exp. 5). There appears to be two maxima in the positive tendency areas in the developing cases. One is approximately at 700 mb, the second appears near the surface. Notice that a negative tendency region surrounds the net positive tendency area, especially in Exp. 1, and to a lesser extent in Exps. 6 and 4. There is no such noticeable concentration of tendency in the non-developing case (Exp. 5). This indicates that, already at 24 h in Exps. 1, 4 and 6, a spin-up mechanism existed whereby the scale of the initial disturbance was reduced from wave scale to depression scale.

The net vorticity tendencies at 48 h, shown in the right side of Fig. 10, clearly show a net increase near the center in Exps. 6 and 1 with maximum magnitudes of 7.6×10^{-9} and 4.0×10^{-9} s^{-2}, respectively. Note the protrusion of positive tendency above level 4 (~335 mb) surrounded by a generally negative region. This is consistent with the development of the generally anticyclonic curvature in the upper-level streamline pattern surrounding the small region of cyclonic curvature (see Fig. 9). In the westerly vertical shear case (Exp. 5) there is a region of small net positive tendency in the lower levels near the disturbance center which is consistent with the intensification of the wave into a weak depression during this time (see Figs. 5 and 6). The negative tendency ahead of the center in Exp. 5 is larger than the positive tendency near the disturbance center. The positive tendency for Exp. 4 in Fig. 10 is very weak. As one can see in Fig. 5, the disturbance in Exp. 4 moves northwestward after 48 h. Accordingly,

TABLE 1. Summary of results at 96 h for Experiments 1, 4, 5 and 6.

	Exp. 1	Exp. 4	Exp. 5	Exp. 6
Four-day longitudinal movement (deg)	24.0	20.1	15.7	35.2
Maximum surface winds (m s^{-1})	17.8	10.4	10.0	22.5
Central surface pressure (mb)	1002.6	1006.2	1006.9	993.5
Magnitude of warm anomaly (K) at level 4 (~335 mb)	3.3	2.1	no warm anomaly	4.4
Maximum vorticity at level 9 (~950 mb) (10^{-6} s^{-1})	237	175	63	365

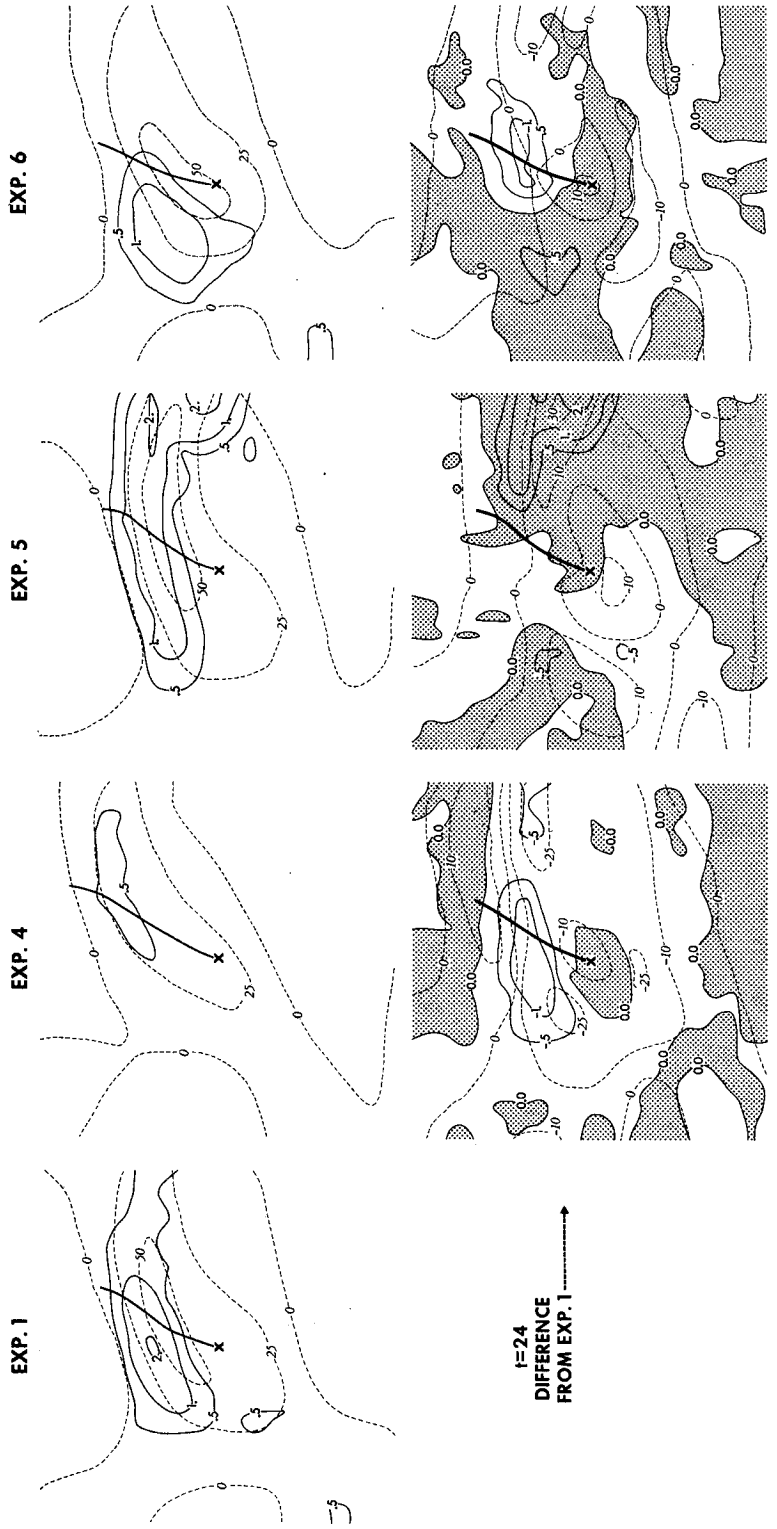

FIG. 7. Distribution at 24 h of rainfall intensity (solid line, mm h^{-1}) and level 9 ($\sigma = 0.95$) vorticity (broken line, 10^{-6} s^{-1}) in Exps. 1, 4, 5 and 6 (top part of figure). Differences from Exp. 1 of rainfall (solid line, mm h^{-1}) and level 9 vorticity (broken line, 10^{-6} s^{-1}) for Exps. 4, 5, 6 (bottom part of figure). Shaded areas indicate positive rainfall departures from Exp. 1. Heavy solid lines indicate surface trough positions and cross marks indicate locations of surface pressure minimum.

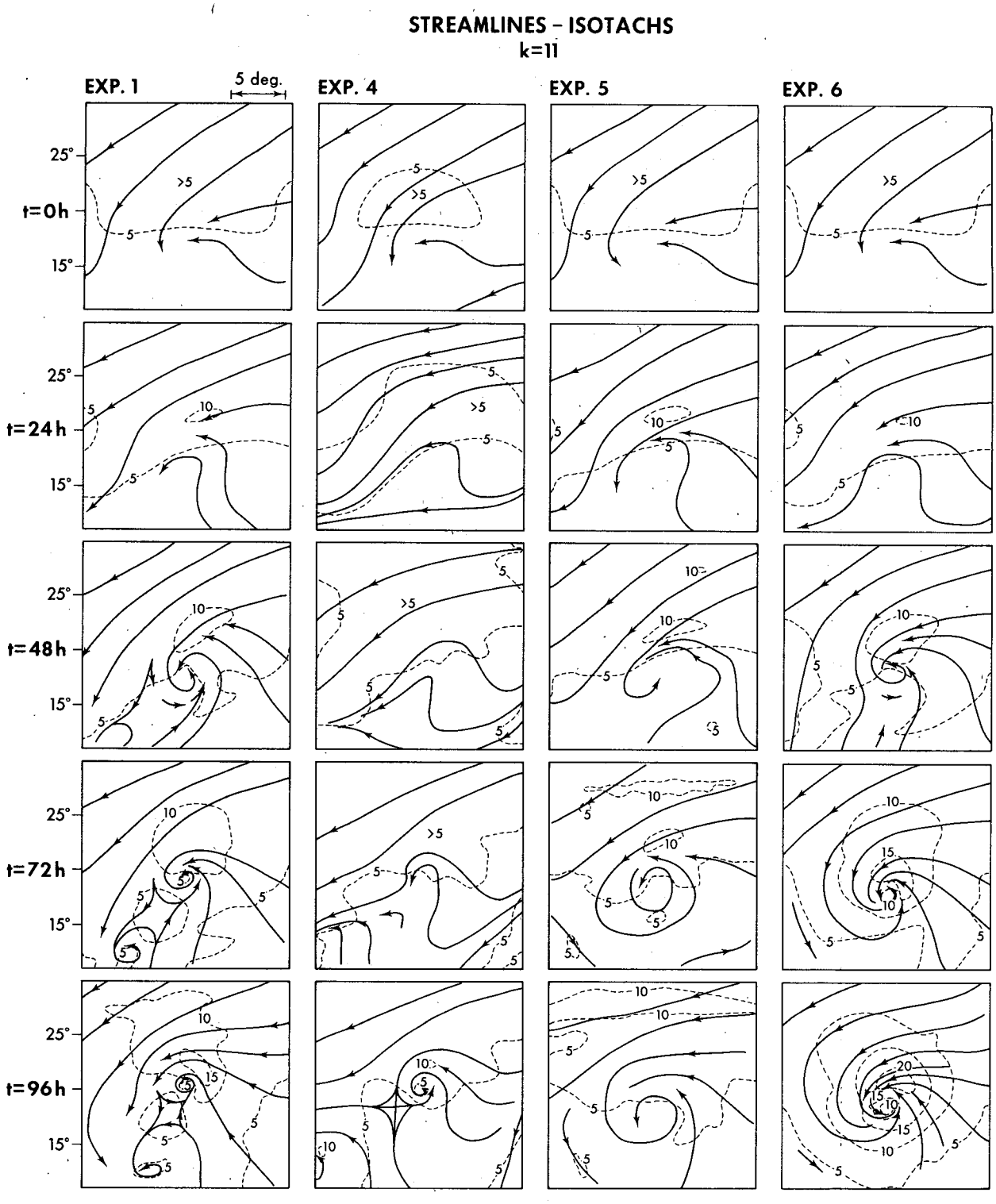

FIG. 8. Streamlines and isotachs (m s^{-1}) at level 11 (σ = 0.992) for Exps. 1, 4, 5 and 6 (from left column to right) at 0, 24, 48, 72 and 96 h (from top to bottom row).

a meaningful part of the tendency field may be missing in the present west–east cross section.

Individual terms of the vorticity budget were analyzed and presented in KT for Exp. 1, and similar analyses were made for Exps. 4, 5 and 6. It was found that the relative importances of each vorticity budget

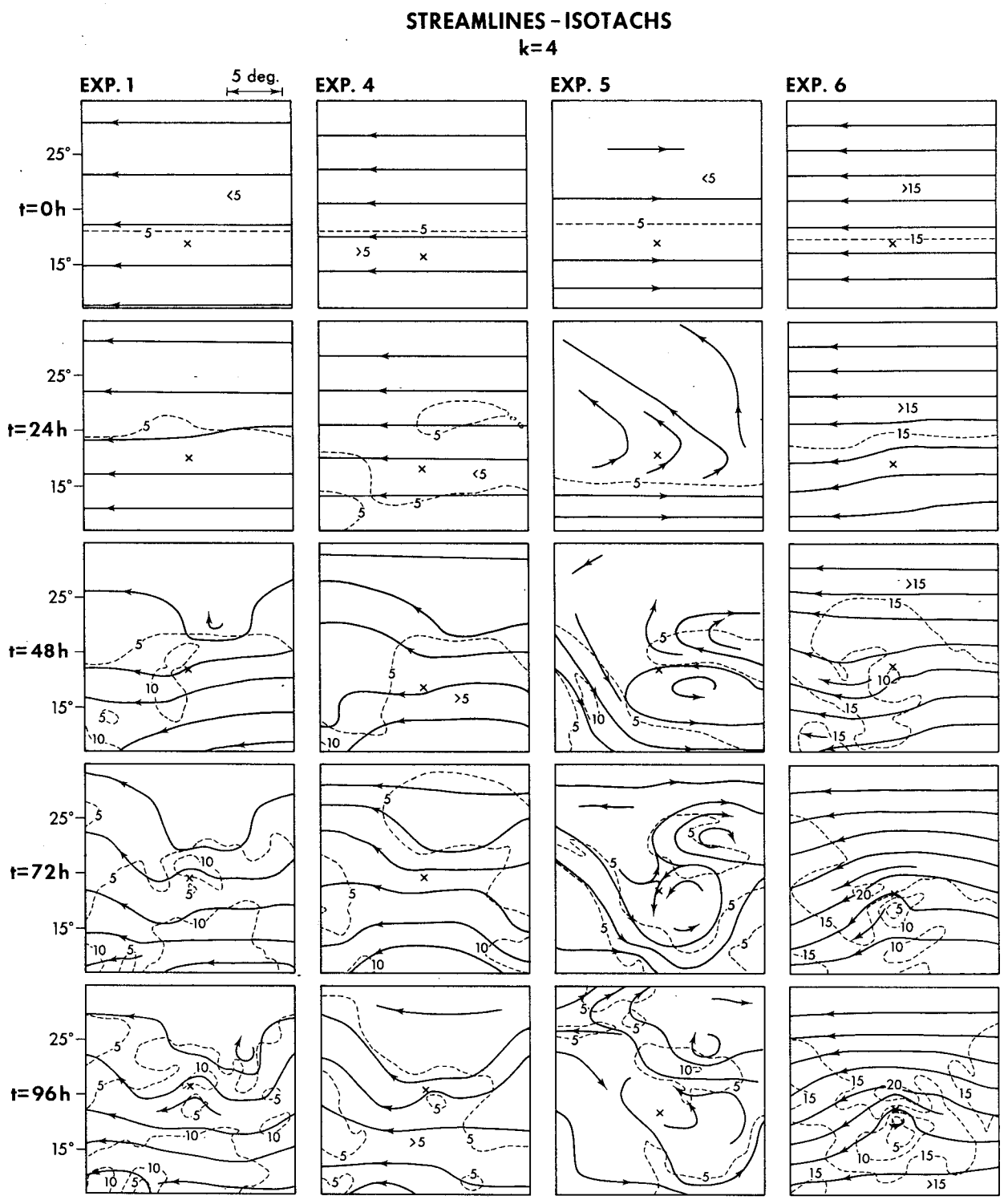

FIG. 9. Streamlines and isotachs (m s^{-1}) at level 4 (σ = 0.335) for Exps. 1, 4, 5 and 6 (from left column to right) at 0, 24, 48, 72 and 96 h (from top to bottom row) Cross marks indicate locations of surface pressure minimum.

term are similar for each experiment. At low levels, the major contributions are made by the stretching, horizontal relative advection, and frictional dissipation terms. At upper levels, horizontal relative advection, stretching and vertical advection of low-level vorticity are important. The twisting effect, of

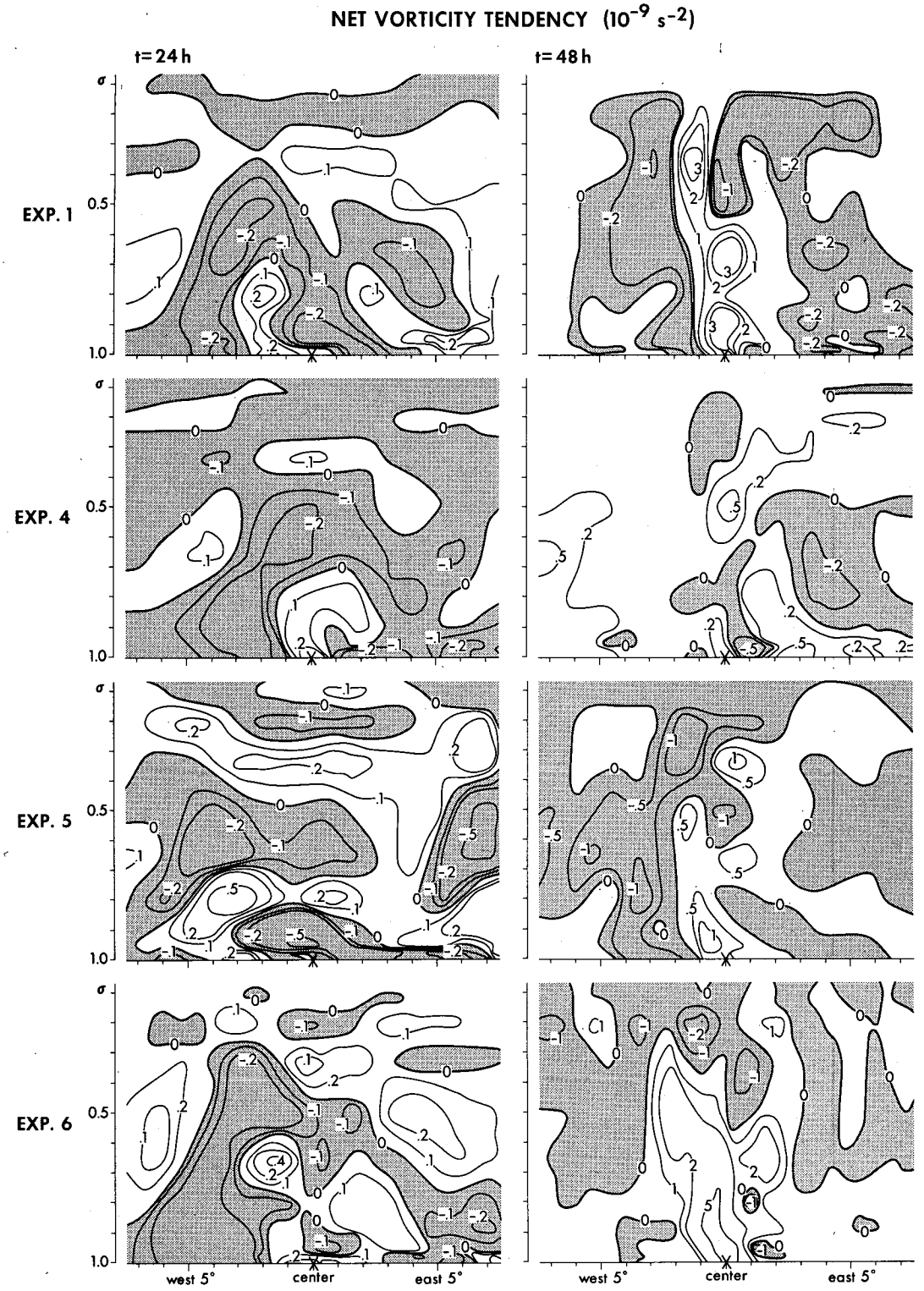

FIG. 10. Longitude-height distribution, through the disturbance center, of the rate of vorticity change (10^{-9} s^{-2}), computed relative to the moving disturbance in Exps. 1, 4, 5 and 6 (top to bottom row) at 24 (left column) and 48 h (right column).

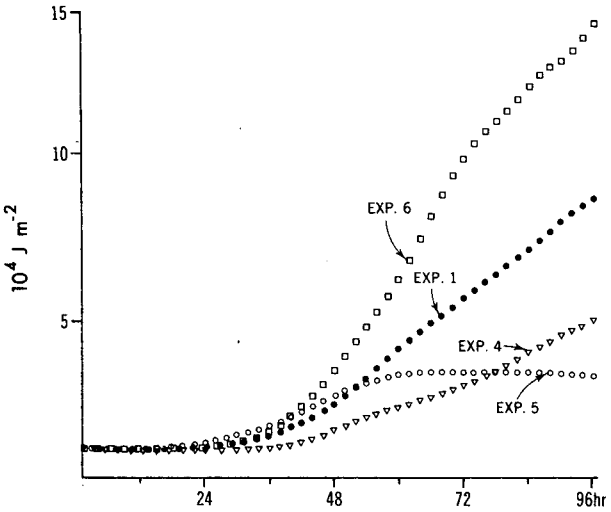

FIG. 11. Time variation of domain-average, eddy kinetic energy in Exps. 1, 4, 5 and 6.

course, is dependent on the vertical shear of the horizontal wind and the horizontal variation of vertical motion. The twisting effect above the incipient disturbance is larger negative in Exp. 6 than 1. In Exp. 5, the twisting effect is small positive aloft.

b. Heating tendencies

The net heating tendencies at 48 h were analyzed for Exps. 1, 4, 5 and 6. It was found that the warming tendency above the developing depression results mainly from a delicate imbalance between the heating due to condensation of water vapor and the opposing cooling effect of upward motion, as mentioned in KT. The relative horizontal advection and the radiational effect also play an important role despite the generally small magnitudes, contributing ~10% of the net tendency above the depression at 48 h. At 48 h, relative advection of heat, which may be called the ventilation effect, in Exps. 1 and 6 is positive aloft ahead of the moving disturbance. In Exp. 5, however, a small positive effect of relative advection was found to the north of the disturbance center.

c. Eddy kinetic energy

The time history of the average eddy kinetic energy in the integration domain was computed for the four experiments and is shown in Fig. 11. It is defined as $\overline{(u'^2 + v'^2)/2}$, where u and v are the longitudinal and latitudinal velocity components, the primes refer to deviations from zonal means, i.e., $u = \bar{u} + u'$, etc., and the double overbar refers to a volume mean. In Exps. 1 and 6, the eddy kinetic energy increases from $\sim 1 \times 10^4$ J m^{-2} initially to 8×10^4 and 15×10^4 J m^{-2} at 96 h, respectively. In Exp. 5, the westerly shear case, the eddy kinetic energy increases for 60 h to 4×10^4 J m^{-2}, then remains relatively constant thereafter. The eddy kinetic energy in Exp. 4 increases to 5×10^4 J m^{-2} mostly in the last 48 h of the experiment. The time tendencies of the eddy kinetic energy of these four experiments roughly parallels the time history of the maximum surface wind shown in Fig. 6. This indicates that the major contribution of the volume mean eddy kinetic energy is made by the disturbance itself and not by other unassociated eddies. Therefore, it is useful to look at a few pertinent terms of the total eddy kinetic energy budget to study the energetics of the disturbances.

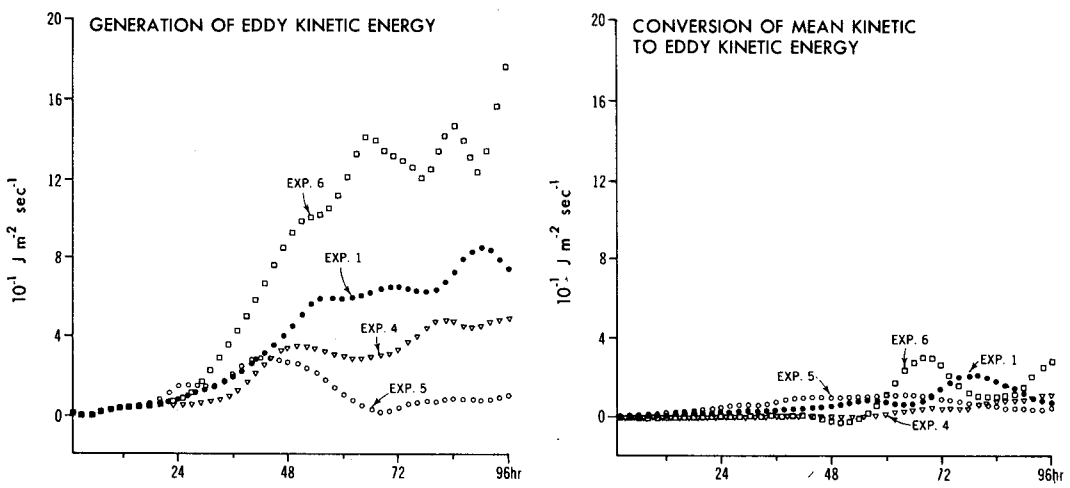

FIG. 12. Time variation of domain-average, generation of eddy kinetic energy in Exps. 1, 4, 5 and 6 (left). Time variation of domain average, conversion of mean kinetic to eddy kinetic energy in Exps. 1, 4, 5 and 6 (right).

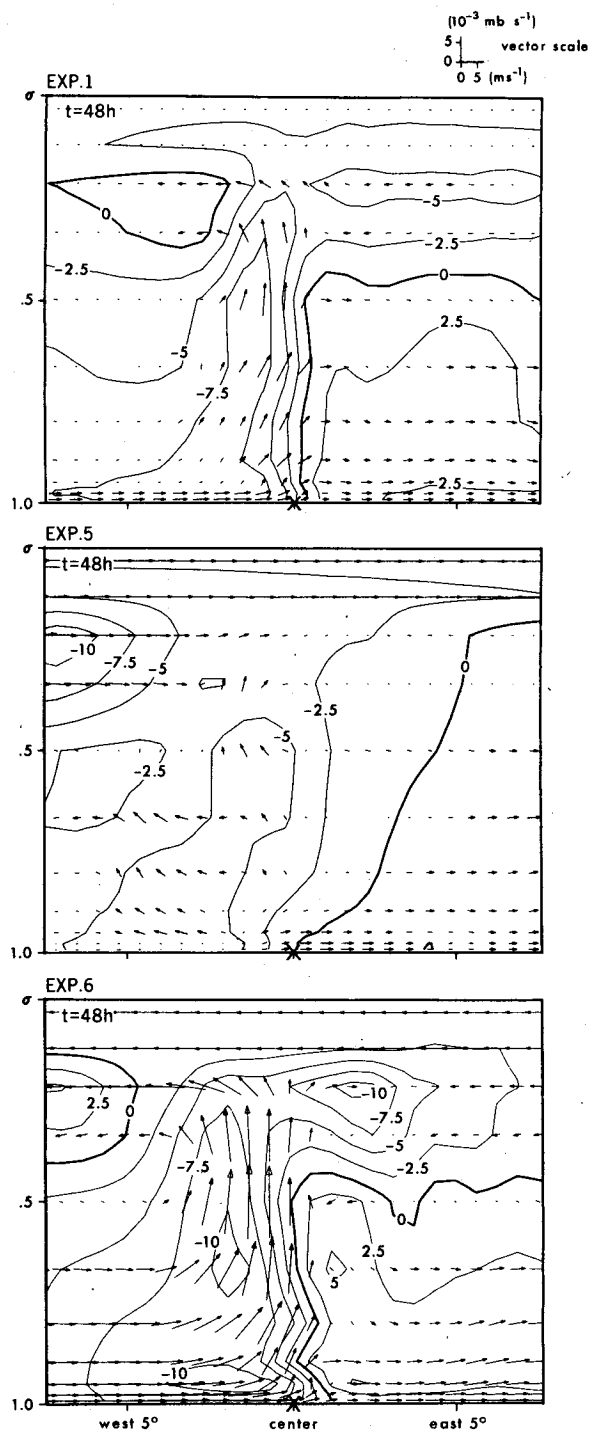

FIG. 13. Longitude-height distribution, through the disturbance center, of the wind relative to the moving system, at 48 h, for Exps. 1, 5 and 6 (top to bottom). Arrows represent the zonal and vertical components and isopleths show distribution of the meridional component (m s^{-1}).

The volume average generation of eddy kinetic energy and the conversion of mean kinetic energy to eddy kinetic energy were computed for Exps. 1, 4, 5 and 6 and are displayed in Fig. 12. The generation of eddy kinetic energy is defined as $-\overline{\overline{\mathbf{v}'\cdot\nabla\phi'}}$, where $\mathbf{v}'$ is the deviation of the vector wind $\mathbf{v}$ from the zonal mean $\bar{\mathbf{v}}$, and $\nabla\phi'$ refers to the deviation of the pressure gradient $\nabla\phi$ from its zonal mean. Again, the double overbar refers to a volume mean. The conversion of mean kinetic to eddy kinetic energy may be defined as

$$-\overline{\overline{v'u'}}\frac{\partial\bar{u}}{\partial y}-\overline{\overline{v'v'}}\frac{\partial\bar{v}}{\partial y}-\overline{\overline{\omega'u'}}\frac{\partial\bar{u}}{\partial p}-\overline{\overline{\omega'v'}}\frac{\partial\bar{v}}{\partial p},$$

where pressure p is the vertical coordinate, ω the vertical velocity in pressure coordinates, and the volume average is taken. Except for Exp. 5, the generation term is much more significant than the conversion term, especially after 48 h. It was found from the budget analyses of eddy available potential energy that the positive contribution of the generation term for all experiments can be linked primarily to the production of eddy available potential energy due to the latent energy release rather than that due to baroclinic instability. The conversion of mean kinetic energy into eddy kinetic energy in Exps. 1 and 6 plays only a minor direct role in intensification of the disturbances. Note, however, the nondeveloping quasi-steady depression of Exp. 5 derives about an equal amount of energy from the mean flow and from eddy available potential energy. This indicates that waves and weak depressions over the ocean can be maintained by a combination of energy supplies through barotropic processes and latent heat release.

6. The effect of vertical shear of the environmental wind on tropical storm genesis

We have analyzed the model tropical storm genesis in Exps. 1 and 6 and the non-genesis in Exp. 5. The vertical shear in these experiments plays quite an important role. With little shear or easterly vertical shear of the basic flow, development of the initial disturbance occurred (Exps. 1 and 6), while with westerly vertical shear, development was suppressed (Exp. 5). In this section, we discuss first the role of the vertical shear in the genesis mechanism through the further analyses of Exps. 1, 5 and 6. Then, based on the six experiments in series A (see Fig. 3), we make a general assessment of the impact of vertical shear on the intensity of the disturbances.

Fig. 13 shows the longitude-height distributions of the flow relative to the moving disturbances at 48 h for Exps. 1, 5 and 6. These and other vertical cross sections are through the center of the disturbances. The solid lines in the figure show the meridional component of the relative wind, while the vectors indicate the longitudinal and vertical components.

It is found in Fig. 13 that a deep, organized radial-vertical circulation is already established at 48 h in Exp. 1. In this circulation, the low-level radial inflow

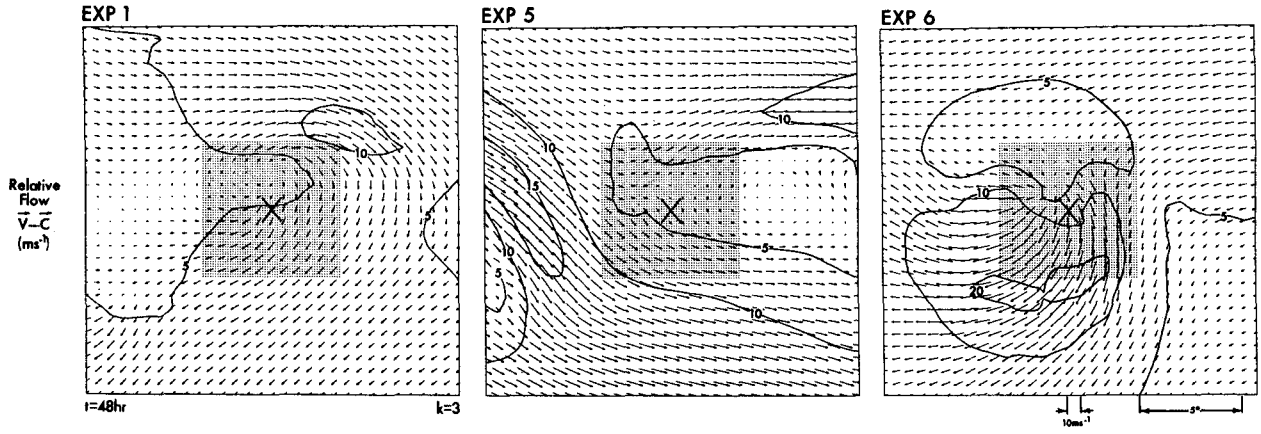

FIG. 14. Distribution of relative wind vector and speed (m s^{-1}) at level 3 (σ = 0.215) for Exps. 1, 5 and 6 (right to left) at 48 h. Shaded area is defined as immediate storm environment.

ahead of the center provides the moisture necessary to maintain heavy condensation heating in the central region, while the upper-level radial outflow yields mass divergence and subsequent deepening of the depression. In the easterly shear case (Exp. 6) the circulation of the aforementioned type is enhanced as seen in Fig. 13. The phase speed of the disturbance in Exp. 6 is significantly larger than Exp. 1 (see Fig. 5). This causes stronger and deeper relative inflow ahead of the center since the basic winds at low levels in Exps. 6 and 1 are about the same. This increased inflow results in intense ascending motion which interacts with the strong upper-level easterly flow to yield the enhanced outflow ahead of the disturbance. In the westerly vertical shear case (Exp. 5) the opposite effects to those mentioned above are observed in Fig. 13. The relative horizontal winds at low levels near the center at 48 h in Exp. 5 are divergent and a relative inflow exists at the upper levels ahead of the center. It is interesting to note that the axis of the disturbance, which may be defined by the zero-contour of the relative meridional flow, tilts to the east with height in Exp. 5 while it is vertical in Exps. 1 and 6.

A horizontal view of the relative flow at level 3 (~215 mb) around the disturbances in Exps. 1, 5 and 6 is shown in Fig. 14. The developing disturbances of Exps. 1 and 6 exhibit anticyclonic, divergent outflow, but, in the non-developing disturbance of Exp. 5, the flow is more convergent and resembles that around a solid cylinder. Note that the initial flow was simply zonal at level 3 in all cases. In Exps. 5 and 6, the vertical shear in the vicinity of the disturbance has been reduced from the initial shear by 48 h. The mean zonal wind shears at 48 h between level 3 (~215 mb) and level 9 (~950 mb) in the shaded area (7° × 7°) in Fig. 14 are −3.30, +3.64 and −6.07 m s^{-1} in Exps. 1, 5 and 6 respectively. Thus, the developing cases exhibit easterly vertical shear in the immediate environment of the disturbance. Williams and Gray (1973) found that prestorm cloud clusters of the Pacific are generally associated with easterly vertical shear.

To study further the effect of vertical shear of the initial basic flow on the evolution of easterly waves, series A experiments were performed [see Fig. 3: in series A, u_1 in (3.1) is fixed at 3.75 m s^{-1} and $u_0(1) = -5$ m s^{-1}]. In each experiment the initial basic low-level flow is easterly and identical to Exp. 1, but different vertical shears are specified. Exps. 5 and 6 are part of this series. The specified values of the initial vertical wind shear ranged from −22.5 (easterly) to +15.0 m s^{-1} (westerly) between σ = 0.15 to σ = 0.85. Fig. 15 illustrates the degree of intensification of the disturbance in 96 h for the specified range of vertical shears. The maximum surface wind speed, the level 9 (σ = 0.95) maximum vorticity, the central surface pressure, and the temperature anomaly at level 4 (σ = 0.335), at 96 h, are used as intensification indicators. The temperature anomaly is defined as the temperature difference between the maximum and minimum temperature at a latitude near the storm center. A clear, systematic pattern emerges, which again indicates a bias toward moderate easterly vertical shear being conducive for development. A large value of easterly vertical shear, however, is detrimental to genesis. The present study implies an alteration of the findings of Palmén (1956), Ramage (1959), Gray (1968) and McBride and Zehr (1981), which suggest a small vertical wind shear with no directional bias is required for development. Landers (1963) observed that tropical storms originated in the regions of easterly vertical shear between 1000 and 500 mb. Climatologically, the genesis area of tropical cyclones include regions with easterly shear such as parts of the Bay of Bengal, the western and eastern Pacific, and the equatorial Atlantic during the tropical cyclone season. On the

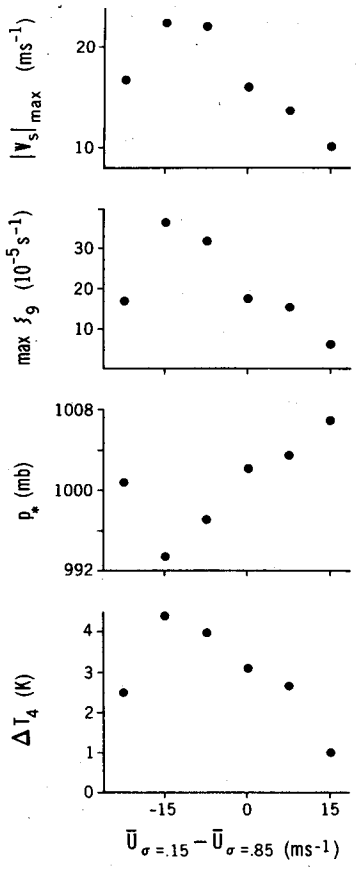

FIG. 15. Graph of disturbance intensity versus environmental vertical wind shear (~150–~850 mb) in series A in which u_1 = 3.75 m s^{-1} and u_0 (1) = −5 m s^{-1} in (3.1). Maximum surface wind, maximum level 9 vorticity, central surface pressure and magnitude of warm anomaly at level 4 (from top to bottom) are used as indicators of intensity.

other hand, westerly shear greater than 10 m s^{-1} between 200 and 850 mb does not exist in any genesis area (Gray, 1968).

It was mentioned previously in this section that the deep radial-vertical circulation of a tropical depression as shown in Fig. 13 for Exp. 1 may be intensified under easterly vertical shear. In the following, we discuss the function of vertical shear of the basic flow in the formation of such a radial-vertical circulation at a much earlier stage (0–24 h) of the model integration. As suggested from the analysis results in KT for Exp. 1, the above circulation is tied to the formation of a relatively warm area at the upper levels as well as to the moisture convergence at the low levels. If these two events are coupled strongly in the vertical, then the intensification of the radial-vertical circulation through a feedback process may be expected. In other words, the genesis of a tropical storm requires that the upper-level warm area remain nearly in phase with the low-level disturbance. As a measure of the degree of coupling at the early stage, we compare the average zonal wind at level 4 (~335 mb), which represents the movement of the upper-level warm air, against the longitudinal phase speed of the low-level disturbance c. In Table 2, $\bar{u}_4 - c$ at 12 h, together with c, $\bar{u}_4$, $\bar{u}_8$ and $\bar{u}_8 - c$, for each experiment in series A are listed. By making an interpolation to the data in Table 2, one sees that the quantity $|\bar{u}_4 - c|$ at 12 h is minimum at a vertical wind shear of approximately −8.25 m s^{-1}, indicating that maximum coupling occurs preferentially for cases with easterly vertical wind shear.

The abovementioned coupling becomes meaningful only when a sufficiently large convergence of latent energy to the low-level disturbance occurs. It seems that the strong low-level wind relative to the moving disturbance tends to cause a large convergence. The parameter $|\bar{u}_8 - c|$ may be taken as a measure of strength of such a relative flow. Table 2 indicates that, in the case of series A experiments, $\bar{u}_8 - c$ increases with easterly vertical shear. (A positive value of $\bar{u}_8 - c$ suggests that the disturbance moves westward faster than the low-level easterlies and, hence, the low-level moist air ahead of the moving disturbance is taken into the disturbance.) In addition, strong low-level winds have a direct positive impact on sea surface evaporation and hence, the moisture supply to an incipient disturbance. In the experiments with strong winds aloft, this momentum is eventually (within ~2 days) transferred to the low-level environment by subsidence and vertical mixing and one would thus expect stronger development. This, together with a large relative inflow, explains why maximum development occurs at a −15 m s^{-1} vertical wind shear, whereas the coupling is more complete at ~ −8 m s^{-1} shear. According to the water vapor budget analysis, at 60 h into the integration, the mean moisture convergence below ~600 mb over the 7° × 7° disturbance area is 1.8, 1.0 and 0.5 × 10^{-4} g kg^{-1} s^{-1} for easterly vertical shears of −15.0, −7.5 and 0.0 ms^{-1}, respectively. For approximately the first 2.5 days, the disturbance embedded in an easterly shear of −7.5 m s^{-1}, i.e., the case of

TABLE 2. Series A disturbance phase speeds, mean zonal wind and relative flow at 12 h for different values of initial vertical shear.

	Easterly shear				Westerly shear	
Vertical shear at 0 h m s^{-1}/(150–850 mb)	−22.5	−15.0	−7.5	0	7.5	15.0
Longitudinal phase speed (m s^{-1}) at 12 h, c	−12.3	−11.0	−9.8	−8.6	−7.4	−5.9
Mean zonal wind (m s^{-1}) at 12 h, at level 4 (~335 mb), $\bar{u}_4$	−19.0	−14.0	−9.3	−5.4	−2.0	2.2
Mean zonal wind (m s^{-1}) at 12 h, at level 8 (~895 mb), $\bar{u}_8$	−6.0	−5.5	−5.0	−4.6	−4.6	−4.5
($\bar{u}_4 - c$) at 12 h (m s^{-1})	−6.7	−3.0	0.5	3.2	5.4	8.1
($\bar{u}_8 - c$) at 12 h (m s^{-1})	6.3	5.5	4.8	4.0	2.8	1.4

nearly complete coupling, is more intense than that of any other series A experiment.

Other possible mechanisms that would prefer easterly vertical shear for development of a disturbance embedded in surface easterlies are those mechanisms which are represented by the twisting term $-\nabla\omega \times \partial v/\partial p$ in the vorticity equation and by the differential vertical advection term $-\nabla\omega \cdot \partial v/\partial p$ in the divergence equation. In the case of easterly vertical shear, the twisting of the horizontal component of vorticity, $\partial\bar{u}/\partial z$, by the maximum upward motion north of the disturbance center, causes anticyclonic flow above the center. In an analogous manner cyclonic flow would develop through twisting above the disturbance center in westerly vertical shear. The differential vertical advection of momentum creates divergence west of the maximum upward motion area with easterly vertical shear and convergence west of the maximum upward motion with westerly shear. The alterations of the upper-level flow through twisting and differential vertical advection effects are suggested by Figs. 9, 10, 13 and 14. In as far as anticyclonic flow above and upper-level divergence ahead of the low-level disturbance is favorable for genesis, the above mechanisms would selectively augment an incipient disturbance in an environment of easterly shear.

In summary, a bias toward easterly vertical shear of the environmental winds in tropical storm genesis occurs in the present model experiments when the mean surface wind is easterly. This directional bias is apparently related to the intrinsic westward phase velocity of the wave disturbance. The phase velocity of a low-level disturbance is a complicated function of many factors including the magnitude, shear, and sign of the basic flow, as well as the depth and horizontal extent of the wave. In an additional experiment with a low-level disturbance embedded in surface westerlies, but with an easterly shear identical to Exp. 6, little development ensued. The phase speed of the disturbance in the above case was such that the coupling with the upper-level flow was weak.

7. The effects of the basic horizontal wind and its shear

a. Horizontal shear of the basic environmental wind

To isolate the effects of different horizontal wind shears on genesis, series B and C experiments were performed. Series B [see Fig. 3: in series B, u_0 in (3.1) is fixed at -5 m s^{-1}] is designed to study the significance of upper-level anticyclonic shear and the lower-level cyclonic shear of the basic flow on tropical storm genesis. In series B, alterations of the basic flow in the developing case (Exp. 1) were made by removing the upper-level anticyclonic shear, the low-level cyclonic shear or both. Table 3 summarizes series B results. The elimination of the anticyclonic shear aloft reduces the strength of the disturbance. The impact, however, is relatively small with the maximum vorticity at level 9 ($\sim$950 mb) decreasing from 237×10^{-6} s^{-1} to 222×10^{-6} s^{-1}. The maximum surface wind is also reduced from 17.8 to 15.9 m s^{-1}. A similar result is indicated between the two experiments in which no initial low-level horizontal shear of the environmental flow was prescribed. Table 2 clearly shows a significant positive contribution of the low-level cyclonic shear of the initial basic flow to storm genesis. When it is removed from Exp. 1, the maximum surface wind at 96 h decreases to 10.1 m s^{-1} compared to 17.8 m s^{-1} in Exp. 1, and the magnitude of the warm core anomaly is 1.9 K, compared to 3.3 K in Exp. 1. To summarize, the Exp. 1 simulation is intense mainly because of the specified initial low-level cyclonic shear of the basic flow, although the basic anticyclonic shear aloft also has a positive impact on disturbance intensification.

TABLE 3. Series B disturbance intensities at 96 h.

Low-level horizontal shear		Upper-level horizontal shear: Anticyclonic $u_1 = -3.75$ m s^{-1}	Upper-level horizontal shear: No shear $u_1 = 0$
		(Exp. 1)	
Cyclonic $u_1 = 3.75$ m s^{-1}	Initial vorticity (10^{-6} s^{-1})	43	43
	Final vorticity (10^{-6} s^{-1})	237	222
	Maximum surface winds (m s^{-1})	17.8	15.9
	Central surface pressure (mb)	1002.6	1003.5
	Magnitude of warm anomaly (K)	3.3	3.0
			(Exp. 4)
No shear $u_1 = 0$	Initial vorticity (10^{-6} s^{-1})	31	31
	Final vorticity (10^{-6} s^{-1})	190	175
	Maximum surface winds (m s^{-1})	10.1	10.4
	Central surface pressure (mb)	1005.9	1006.2
	Magnitude of warm anomaly (K)	1.9	2.1

Table 4 summarizes the results from the series C experiments. In series C, a vertically invariant, horizontal basic flow was prescribed as an initial condition (see Fig. 3). As in series B, the uniform part of the basic flow was fixed at ~ -5 m s^{-1}. Generally, as the basic shear changes from anticyclonic to cyclonic, an increase in intensity occurs. Even though

TABLE 4. Series C disturbance intensities at 96 h.

	Horizontal shear (uniform with height): Anticyclonic $u_1 = -3.75$ m s^{-1}	No shear $u_1 = 0$	Cyclonic $u_1 = 3.75$ ms^{-1}
		(Exp. 4)	
Initial vorticity (10^{-6} s^{-1})	18	31	43
Final vorticity (10^{-6} s^{-1})	17	175	175
Maximum surface winds (m s^{-1})	5.5	10.4	16.2
Central surface pressure (mb)	1008.1	1006.2	1002.1
Magnitude of warm anomaly (K)	0.6	2.1	3.1

TABLE 5. Series D disturbance intensities at 96 h and upper- and lower-level mean zonal flows and disturbance phase speeds at 12 h.

	Uniform flow u_0		
	-5 m s^{-1} (Exp. 4)	0 m s^{-1} (no basic flow)	5 m s^{-1}
Initial vorticity (10^{-6} s^{-1})	31	31	32
Final vorticity (10^{-6} s^{-1})	175	122	284
Maximum surface winds (m s^{-1})	10.4	9.6	14.9
Central surface pressure (mb)	1006.2	1006.5	999.2
Magnitude of warm anomaly (K)	2.1	1.4	2.7
Longitudinal phase speed (m s^{-1}) at 12 h, c	-8.6	-2.9	5.7
Mean zonal wind (m s^{-1}) at 12 h, at level 4 ($\sim$335 mb), $\bar{u}_4$	-4.9	0.0	4.7
Mean zonal wind (m s^{-1}) at 12 h, at level 8 ($\sim$895 mb), $\bar{u}_8$	-4.7	0.1	4.8
($\bar{u}_4 - c$) at 12 h (m s^{-1})	3.7	2.9	-1.0
($\bar{u}_8 - c$) at 12 h (m s^{-1})	3.9	3.0	-0.9

the specified initial perturbation strength is identical in all three experiments, the final vorticity of the disturbance in the anticyclonic environment is less than the initial vorticity. In contrast, the intensity increases in the cases of no shear and cyclonic shear. A basic anticyclonic shear throughout the troposphere seems especially detrimental to disturbance intensification. Notice that none of the primary disturbances in series C reached the overall strength of that found in Exp. 1.

b. Uniform horizontal wind

In order to investigate the role of the uniform part of the basic flow, series D experiments were performed. In these experiments u_1 of (3.1) was set to zero, and u_0 was fixed with height. Consequently, there existed neither horizontal nor vertical shear. As seen in Fig. 3, the specified values of u_0 were -5, 0 and 5 m s^{-1}. The results, summarized in Table 5, indicate greater intensification for nonzero uniform basic flow. This may be explained by the greater evaporation from the ocean in the presence of a mean basic flow. Quite surprisingly, however, there is a bias for development toward westerly uniform flow. The intensity at 96 h of the disturbance with west winds, u_0 = 5 m s^{-1}, is not only greater than the other series D experiments, but also approximately the same as Exp. 1. This bias can again be explained by the coupling between the phase speed of the disturbance and the upper-level flow. As can be seen in Table 5, in case of westerly flow, the coupling ($\bar{u}_4 - c$) is more complete than with easterly flow.

Another intriguing aspect of series D is the difference in the structure of the disturbances at 96 h between easterly and westerly environmental flow. Fig. 16, showing the distribution of vorticity at level 9 ($\sim$950 mb) at 96 h, indicates that as the basic environmental wind becomes more westerly, a tendency for a north–south band emanating from the main disturbance increases. The same tendency is noticed in the fields of convergence, vertical motion and rainfall. This storm structure is similar to some observed tropical storms as well as quite similar to the extratropical storm structure in the westerlies. A banded feature which occurred in Tropical Storm Arlene (May, 1981) was similar to Fig. 16 (bottom).[1] In this rare, early-season storm, a relatively uniform westerly environmental flow prevailed. These results also may be relevant to cases when a disturbance moves northward and encounters westerlies, and suggest a possibility that a disturbance may develop under certain conditions in the extratropical westerlies without baroclinicity. Simpson and Pelissier (1971) found disturbances in the Atlantic, which draw energy from both baroclinic and latent energy sources, and called such hybrid systems "neutercanes."

[1] Personal communication with B. Jarvinen of the National Hurricane Center, May 1981.

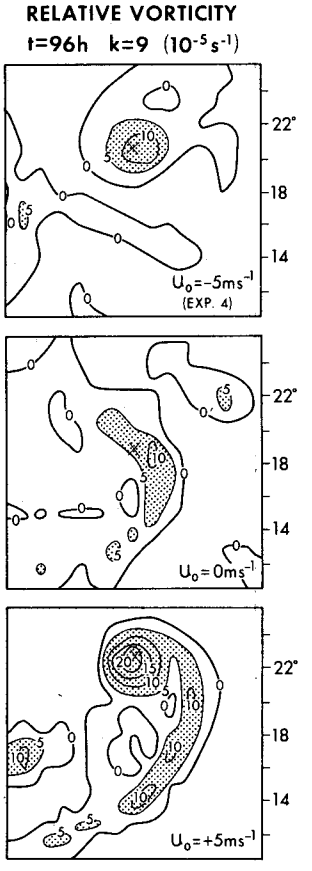

FIG. 16. Distribution of level 9 (σ = 0.95) vorticity (10^{-5} s^{-1}) at 96 h for series D experiments, for $u_0 = -5$, 0 and 5 m s^{-1} (top to bottom), respectively. In series D, environmental flow is uniform, i.e., $u_1 = 0$ in (3.1). Shaded areas indicate values $>5 \times 10^{-5}$ s^{-1}.

The investigation of the mechanism which causes the differences in the structure and phase speed among the vortices in the series D experiments is certainly an interesting subject for future research. An obvious difference between cyclonic vortices embedded in uniform easterly and in uniform westerly flow is the location of the strongest wind relative to the disturbance center. It is to the north (south) of the center in the case of easterly (westerly) environmental flow. Usually the areas of large evaporation, large convergence and, hence, relatively large upward motion are more or less coincident with the area of strong wind. Such distributions affect the rates of change of various quantities. The contrast between the easterly and westerly cases manifests itself in the $u\beta$ term in the divergence equation and also in the $v\beta$ term in the vorticity budget. Specifically, a westerly zonal flow contributes to the increase of convergence south of the disturbance center while this area of convergence may be modified through the $v\beta$ term. Furthermore, the disturbance phase speed, interrelated to the abovementioned asymmetric effects, is dependent on the direction of the uniform flow.

8. Summary and remarks

In this study, the influence of different environmental winds on the genesis of a tropical storm was investigated through the use of a numerical model. In the simulation experiments, the same initial perturbation was superposed on different zonal mean environmental flows. It was found that the degree of dynamic coupling between the low-level disturbance and upper-level flow is a prime indicator of subsequent genesis. The low-level inflow relative to the moving disturbance and the transfer of momentum from aloft into the boundary layer over a large area surrounding the disturbance affect the supply of latent energy and are therefore additional indicators of genesis potential.

In these respects, the vertical shear of the environmental wind plays a vital role in storm genesis. When the mean surface wind is easterly, easterly vertical shear, i.e., easterlies increasing with height, of moderate magnitude is conducive for storm genesis. In one experiment with surface easterlies of -5 m s^{-1} and an easterly vertical shear of -15 m s^{-1} between 150 and 850 mb, the initially specified disturbance developed into a vigorous tropical storm with surface wind exceeding 22 m s^{-1} at 96 h. On the other hand, westerly vertical shear with equivalent magnitude is detrimental to storm development. In an experiment with an initial zonal mean westerly shear of 15 m s^{-1}, the initial disturbance did not intensify beyond the weak depression stage. Except for the vertical shear of the zonal wind, the initial conditions of the above two experiments were identical. It was found that the coupling of the upper troposphere with the moving shallow disturbance is more complete with easterly vertical wind shear. The enhancement of the radial-vertical flow, momentum transfer from aloft and vorticity twisting effects are other possible factors which make easterly vertical shear favorable for storm genesis. However, with westerly surface flow, easterly vertical wind shear is not as conducive for genesis because the phase speed of the disturbance is affected differently and coupling between the upper and lower levels is less complete.

The wave stage horizontal structure of the disturbances were also affected by the vertical wind shear. The vertical velocity and precipitation patterns relative to the trough position were modulated by the direction of the environmental vertical shear. Westerly shear produced a pattern like that of the classic easterly wave (Riehl, 1954) while an easterly shear environment produced a pattern more akin to waves in the equatorial western Pacific (Reed and Recker, 1971).

The effects of horizontal wind and its shear on storm genesis also were investigated. Low-level cyclonic shear of the basic flow exhibited a positive impact on development which is similar to the observations of Gray (1968, 1979) and Hebert (1978). Upper-level anticyclonic shear was also found to have a small, but positive impact on storm development. A surprising result of this study was that of a directional preference of the uniform part of the basic environmental wind. Uniform westerlies were more conducive for storm development than uniform easterlies. Moreover, the low-level storm structure was remarkably different between westerly and easterly uniform flows. The disturbance which evolved in westerly flow had similar vorticity and precipitation patterns to those of extratropical cyclones. These differences are attributable to various factors such as the latitudinal variation of the Coriolis parameter, the low-level convergence patterns and the phase speed of the disturbance.

The experimental design of the present study was intentionally made simple in order to clarify the effects of changes in the basic environmental flow. This strategy worked successfully and many informative results were obtained. In reality, however, a variety of complications arise. For example, the basic environmental flow cannot be construed to be uniform in the zonal direction with no initial meridional component. The zonal variation of the basic flow was found to be important in genesis by Shapiro (1977). Another simplification in this experimental design is the relative isolation of the domain from equatorial or midlatitude effects. Early observations such as Riehl (1950) and Ballenzweig (1959) indicate the possible importance of interaction with midlatitude phenomena. Also, Sadler (1976) discussed the role

of the tropical upper tropospheric trough in the typhoon development. Further investigation of the above subjects is needed through observational analyses and numerical experiments with relaxation of the limitations of the present model.

Finally, it should be kept in mind that the effect of cumulus convection is incorporated in the present model by a parameterization method in which the stability property of the environment is considered. Ignored in this model, and in many other numerical models, is the direct influence of the environmental flow on the convective activity of the clouds, both individually and as a whole. The extent of impact of the above effect on the evolution of meteorological phenomena which involve the moist convective process, including tropical storm genesis, is not yet well understood. Hopefully, these effects will have little impact on the results obtained in this numerical simulation study. The uncertainty of this assumption is an important topic for future research.

Acknowledgments. The authors would like to express their appreciation to J. Smagorinsky and K. Miyakoda of the Geophysical Fluid Dynamics Laboratory for their constant encouragement during this study. They wish to thank R. J. Reed of the University of Washington, L. Shapiro of the National Hurricane Research Laboratory, B. Jarvinen of the National Hurricane Center, and F. B. Lipps and I. Held of the Geophysical Fluid Dynamics Laboratory for many valuable comments on a preliminary version of the manuscript. P. Tunison, W. Ellis, M. Zadworney, J. Conner and J. Kennedy deserve credit for assistance in the preparation of the manuscript.

REFERENCES

Ballenzweig, E., 1959: Relation of long-period circulation anomalies to tropical storm formation and motion. *J. Meteor.*, **16,** 121–139.

Gray, W. M., 1968: Global view of the origin of tropical disturbances and storms. *Mon. Wea. Rev.*, **96,** 669–700.

——, 1979: Hurricanes: their formation, structure and likely role in the tropical circulation. *Meteorology Over The Tropical Oceans,* D. B. Shaw, Ed., Roy. Meteor. Soc., 155–218.

Hebert, P. J., 1978: Intensification criteria for tropical depressions of the western North Atlantic. *Mon. Wea. Rev.*, **106,** 831–840.

Holton, J. R., 1971: A diagnostic model for equatorial wave disturbances: The role of vertical shear of the mean zonal wind. *J. Atmos. Sci.*, **28,** 55–64.

Keshavamurty, R. N., G. C. Asnani, P. V. Pillai and S. K. Das, 1978: Some studies of the growth of monsoon disturbances. *Proc. Indian Acad. Sci.*, **87A,** 61–75.

Kurihara, Y., 1973: A scheme of moist convective adjustment. *Mon. Wea. Rev.*, **101,** 547–553.

——, and M. A. Bender, 1980: Use of a movable nested-mesh model for tracking a small vortex. *Mon. Wea. Rev.*, **108,** 1792–1809.

——, and R. E. Tuleya, 1981: A numerical simulation study on the genesis of a tropical storm. *Mon. Wea. Rev.* **109,** 1629–1653.

Landers, H., 1963: On the formation and development of tropical cyclones. *J. Appl. Meteor.*, **2,** 206–218.

McBride, J. L., and R. Zehr, 1981: Observational analysis of tropical cyclone formation. Part II: Comparison of non-developing versus developing systems. *J. Atmos. Sci.*, **38,** 1132–1151.

Mellor, G. L., and T. Yamada, 1974: A hierarchy of turbulence closure models for planetary boundary layers. *J. Atmos. Sci.*, **31,** 1791–1806.

Palmén, E., 1956: Formation and development of tropical cyclones. *Proc. Trop. Cyclone Symposium,* Brisbane, Australian Bureau of Meteorology, 213–231.

Ramage, C. S., 1959: Hurricane development. *J. Meteor.*, **16,** 227–237.

Reed, R. J., and E. E. Recker, 1971: Structure and properties of synoptic-scale wave disturbances in the equatorial western Pacific. *J. Atmos. Sci.*, **28,** 1117–1133.

Riehl, H., 1950: A model of hurricane formation. *J. Appl. Phys.*, **21,** 917–925.

——, 1954: *Tropical Meteorology.* McGraw Hill, 392 pp.

Sadler, J. C., 1976: A role of the tropical upper tropospheric trough in early season typhoon development. *Mon. Wea. Rev.*, **104,** 1266–1278.

——, and L. K. Oda, 1980: GATE analyses. I. The synoptic (A) scale circulations during Phase I, 26 June–16 July 1974. II. Means for Phases I, II and III. Dept. of Meteor., University of Hawaii, Honolulu, 32 pp.

Shapiro, L. J., 1977: Tropical storm formation from easterly waves: A criterion for development. *J. Atmos. Sci.*, **34,** 1007–1021.

Simpson, R. H., and J. M. Pellissier, 1971: Atlantic hurricane season of 1970. *Mon. Wea. Rev.*, **99,** 269–277.

Sundqvist, H., 1970: Numerical simulation of tropical cyclones with a ten-level model. Part II. *Tellus,* **22,** 504–510.

Williams, K. T., and W. M. Gray, 1973: Statistical analysis of satellite observed trade wind cloud clusters in the western North Pacific. *Tellus,* **25,** 313–336.

Yamasaki, M., 1977: A preliminary experiment of the tropical cyclone without parameterizing the effect of cumulus convection. *J. Meteor. Soc. Japan,* **55,** 11–31.